

RESEARCH

Open Access



# Comprehensive ceRNA network for MACF1 regulates osteoblast proliferation

Shanfeng Jiang<sup>1†</sup>, Chong Yin<sup>1,2,3,4†</sup>, Kai Dang<sup>1,2,3</sup>, Wenjuan Zhang<sup>1,2,3</sup>, Ying Huai<sup>1,2,3</sup> and Airong Qian<sup>1,2,3\*</sup>

## Abstract

**Background** Previous studies have shown that microtubule actin crosslinking factor 1 (MACF1) can regulate osteoblast proliferation and differentiation through non-coding RNA (ncRNA) in bone-forming osteoblasts. However, the role of MACF1 in targeting the competing endogenous RNA (ceRNA) network to regulate osteoblast differentiation remains poorly understood. Here, we profiled messenger RNA (mRNA), microRNA (miRNA), and long ncRNA (lncRNA) expression in MACF1 knockdown MC3TC-E1 pre-osteoblast cells.

**Results** In total, 547 lncRNAs, 107 miRNAs, and 376 mRNAs were differentially expressed. Significantly altered lncRNAs, miRNAs, and mRNAs were primarily found on chromosome 2. A lncRNA-miRNA-mRNA network was constructed using a bioinformatics computational approach. The network indicated that mir-7063 and mir-7646 were the most potent ncRNA regulators and *mef2c* was the most potent target gene. Pathway enrichment analysis showed that the fluid shear stress and atherosclerosis, p53 signaling, and focal adhesion pathways were highly enriched and contributed to osteoblast proliferation. Importantly, the fluid shear stress and atherosclerosis pathway was co-regulated by lncRNAs and miRNAs. In this pathway, *Dusp1* was regulated by AK079370, while *Arhgef2* was regulated by mir-5101. Furthermore, *Map3k5* was regulated by AK154638 and mir-466q simultaneously. AK003142 and mir-3082-5p as well as Ak141402 and mir-446 m-3p were identified as interacting pairs that regulate target genes.

**Conclusion** This study revealed the global expression profile of ceRNAs involved in the differentiation of MC3TC-E1 osteoblasts induced by MACF1 deletion. These results indicate that loss of MACF1 activates a comprehensive ceRNA network to regulate osteoblast proliferation.

**Keywords** Microtubule actin crosslinking factor 1 (*macf1*), Competing endogenous RNA (ceRNA), Osteoblast proliferation, lncRNA, miRNA, Transcriptomic analysis

†Shanfeng Jiang and Chong Yin, these authors contributed equally to this work and should be considered co-first authors.

\*Correspondence:

Airong Qian  
qianair@nwpu.edu.cn

<sup>1</sup>Lab for Bone Metabolism, Xi'an Key Laboratory of Special Medicine and Health Engineering, Key Lab for Space Biosciences and Biotechnology, School of Life Sciences, Northwestern Polytechnical University,

710072 Xi'an, Shaanxi, China

<sup>2</sup>Research Center for Special Medicine and Health Systems Engineering, School of Life Sciences, Northwestern Polytechnical University, 710072 Xi'an, Shaanxi, China

<sup>3</sup>NPU-UAB Joint Laboratory for Bone Metabolism, School of Life Sciences, Northwestern Polytechnical University, 710072 Xi'an, Shaanxi, China

<sup>4</sup>Department of Clinical Laboratory, Academician (expert) workstation, Lab of epigenetics and RNA therapy, Affiliated Hospital of North Sichuan Medical College, 637000 Nanchong, China



## Background

Decreased bone formation plays a major role in osteoporosis, which results in low bone mass and increased fracture risk [1]. New bone formation is primarily mediated by osteoblasts [2, 3]. Therefore, regulating osteoblast proliferation and differentiation can enhance bone formation.

Previous studies have shown that microtubule actin crosslinking factor 1 (MACF1) can regulate osteoblast proliferation and differentiation in bone-forming osteoblasts [4, 5]. MACF1 can bind to actin filaments through its N-terminal calponin homology domain and positively regulates the Wnt/b-catenin signaling pathway, which is involved in multiple stages of osteoblast differentiation and bone formation [6–8]. To date, however, these studies have focused on a single regulator and systematic transcriptome-wide analysis of the MACF1 regulation network, especially the competing endogenous RNA (ceRNA) network, remains limited.

Non-coding RNA (ncRNA) is thought to play an important role in cellular processes. More recently, it has also been suggested that microRNA (miRNA) and long ncRNA (lncRNA) interact with each other, imposing an additional level of post-transcriptional regulation [9–11]. Furthermore, ncRNA and messenger RNA (mRNA) can form a well-regulated ceRNA interaction network. MiRNAs are a relatively well-documented class of ncRNAs involved in the regulation of various biological processes [12–15]. They can cause transcriptional degradation or translational inhibition by post-transcriptional regulation and binding to mature mRNAs. Many miRNAs have been implicated in the regulation of osteogenic differentiation. Mir-27a-3p and mir-365 can enhance osteogenesis in MC3T3-E1 cells, while mir-195, mir-146a, and mir-705 can inhibit this process [16–20]. LncRNAs, the largest class of ncRNAs in the mammalian genome, undergo further alteration by post-transcriptional modification to regulate gene expression [21]. Several studies have indicated that lncRNAs can promote osteoblast proliferation and differentiation by direct regulation of genes. For example, lnc-ob1 regulates osteoblast activity and bone formation in mice by up-regulating the osteogenic transcription factor Osterix [22]. In addition, H19 can act as a competitive inhibitor of mir-141 and mir-22 to reverse their inhibition of Wnt/beta-catenin signaling, thereby promoting osteogenic differentiation [23, 24].

To date, however, few studies have explored the pre-transcriptional levels of ncRNAs involved in osteogenesis. Furthermore, none of these interaction networks have been shown to regulate the MACF1-induced osteoblast proliferation of MC3T3-E1 cells. Analysis of the genetic factors that affect osteoblast proliferation and differentiation will provide valuable insight into bone diseases. In this study, MC3T3-E1 cells, which are precursor

**Table 1** Profiles of DEGs and ncRNAs in MACF1-knockdown cell line

Gene	Total number	Expression	MACF1 <sup>-/-</sup> vs. WT	Ratio
lncRNA	47 047	Up-regulated	369	0.78%
		Down-regulated	268	0.57%
miRNA	1 900	Up-regulated	64	3.37%
		Down-regulated	43	2.26%
mRNA	29 086	Up-regulated	236	0.81%
		Down-regulated	140	0.48%

MACF1<sup>-/-</sup>: MACF1-knockdown cell line, WTL: wide type

cells of osteoblasts, were used to examine the regulation pathways of MACF1. We conducted integrative analysis of the gene expression profiles of mRNAs, miRNAs, and lncRNAs induced by MACF1.

## Results

### Profiles of DEGs and ncRNAs

After applying a stringent filtering approach, we identified 547 differentially expressed lncRNAs in the MACF1-knockdown MC3T3-E1 cells, including 205 up-regulated and 304 down-regulated lncRNAs. We also identified 107 differentially expressed miRNAs, including 64 up-regulated and 43 down-regulated miRNAs, and 376 differentially expressed mRNAs, including 236 up-regulated and 140 down-regulated mRNAs, as presented in the clustering heat map (Fig. 1). Although the number of dysregulated miRNAs was the lowest, miRNAs had a higher ratio of DEGs/identified genes (5.63%) compared to lncRNAs (1.35%) and mRNAs (1.29%) (Table 1). The top three differentially expressed miRNAs were up-regulated mir-6942-3p and down-regulated mir-1950 and mir-669p-3p. AK033832 was the most up-regulated lncRNA and was located on chromosome 1. Locational distributions of the differentially expressed lncRNAs, miRNAs, and mRNAs were analyzed synchronously. The significantly altered lncRNAs, miRNAs, and mRNAs were found at the highest levels on chromosome 2 and at the lowest levels on chromosome Y (Fig. 1). No relatively consistent variation pattern was observed among the aberrant lncRNA and miRNA species. In addition, 25 lncRNAs, four miRNAs, and 14 mRNAs were located on chromosome 4, which was also the location of MACF1.

### Comprehensive functional analysis of genes and ncRNAs

The main functions of the differentially expressed mRNAs were explored using GO annotation and KEGG pathway enrichment analysis (Fig. 2). All enriched biological processes were related to organization, proliferation, migration, and differentiation (Fig. 2). For example, both regulation and negative regulation of epithelial cell proliferation were enriched, and extracellular matrix

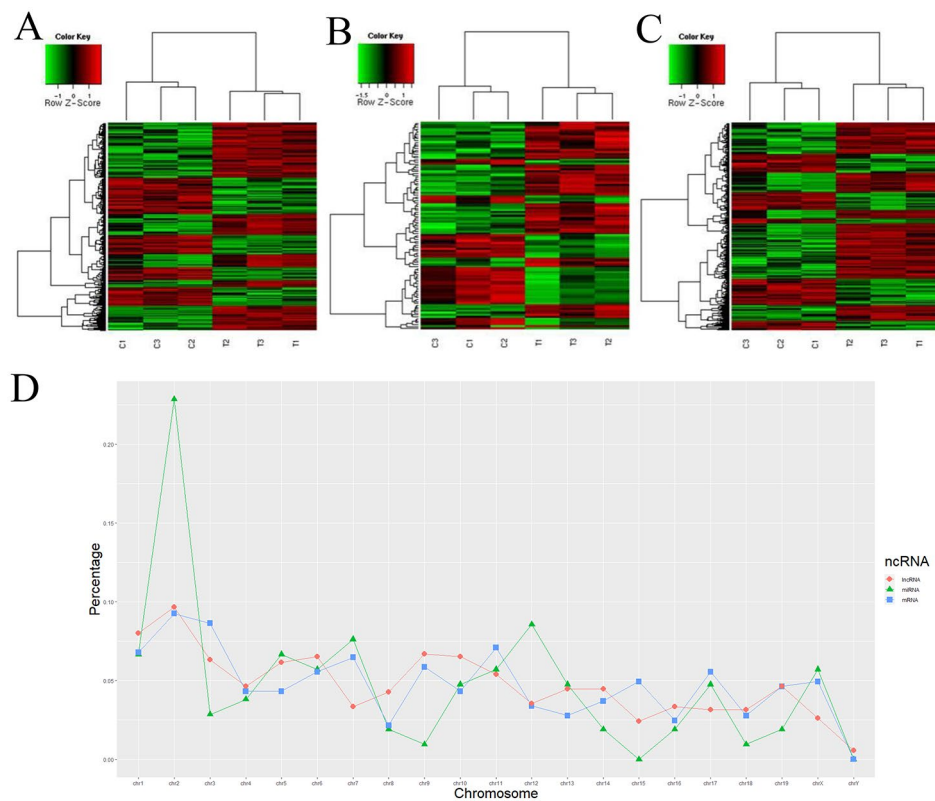


**Fig. 1** The profile of differentially expressed lncRNA, miRNA and mRNA in the MACF1 knockdown. MC3TC-E1 cells. A: Hierarchical cluster analysis of the differentially expressed lncRNAs. The red color represented higher expression, and the green color represented lower expression. B: Hierarchical cluster analysis of the differentially expressed miRNAs. The red color represented higher expression, and the green color represented lower expression. C: Hierarchical cluster analysis of the differentially expressed mRNAs. The red color represented higher expression, and the green color represented lower expression. D: Location distributions of deregulated lncRNAs, miRNA and mRNAs on chromosomes

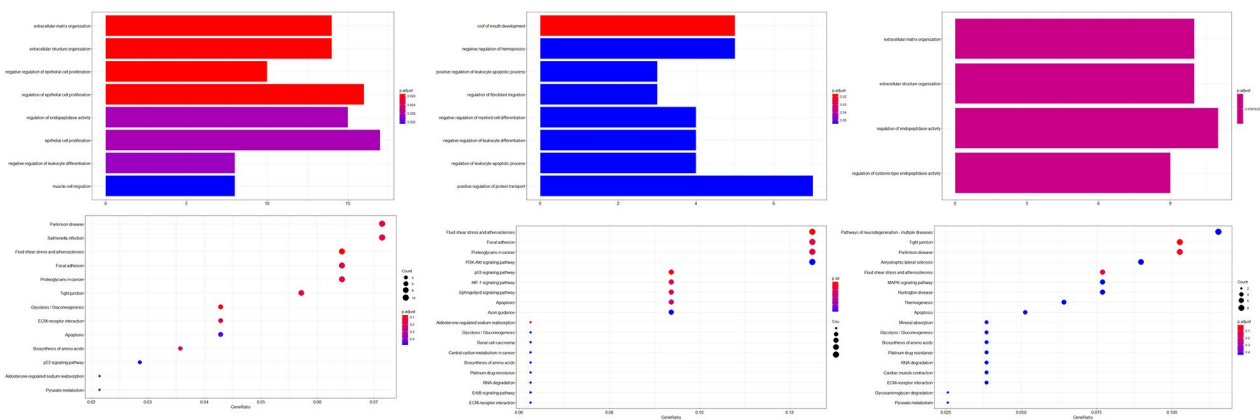


**Fig. 2** Functional enrichment analysis of ceRNAs. A: GO and KEGG analysis of differentially expressed mRNA. B: GO and KEGG analysis of differentially expressed genes targeted by miRNA. C: GO and KEGG analysis of differentially expressed genes targeted by lncRNA.

organization was the most enriched process. For pathway analysis, the fluid shear stress and atherosclerosis, p53 signaling, and focal adhesion pathways, which are involved in osteoblast proliferation [25–29], were all enriched.

For miRNA regulation analysis, biological processes related to migration and differentiation, which are influenced by MACF1 [30, 31], were significantly enriched. Among the miRNAs enriched in KEGG pathways, mir-370 - 3p was predicted to have the greatest number of

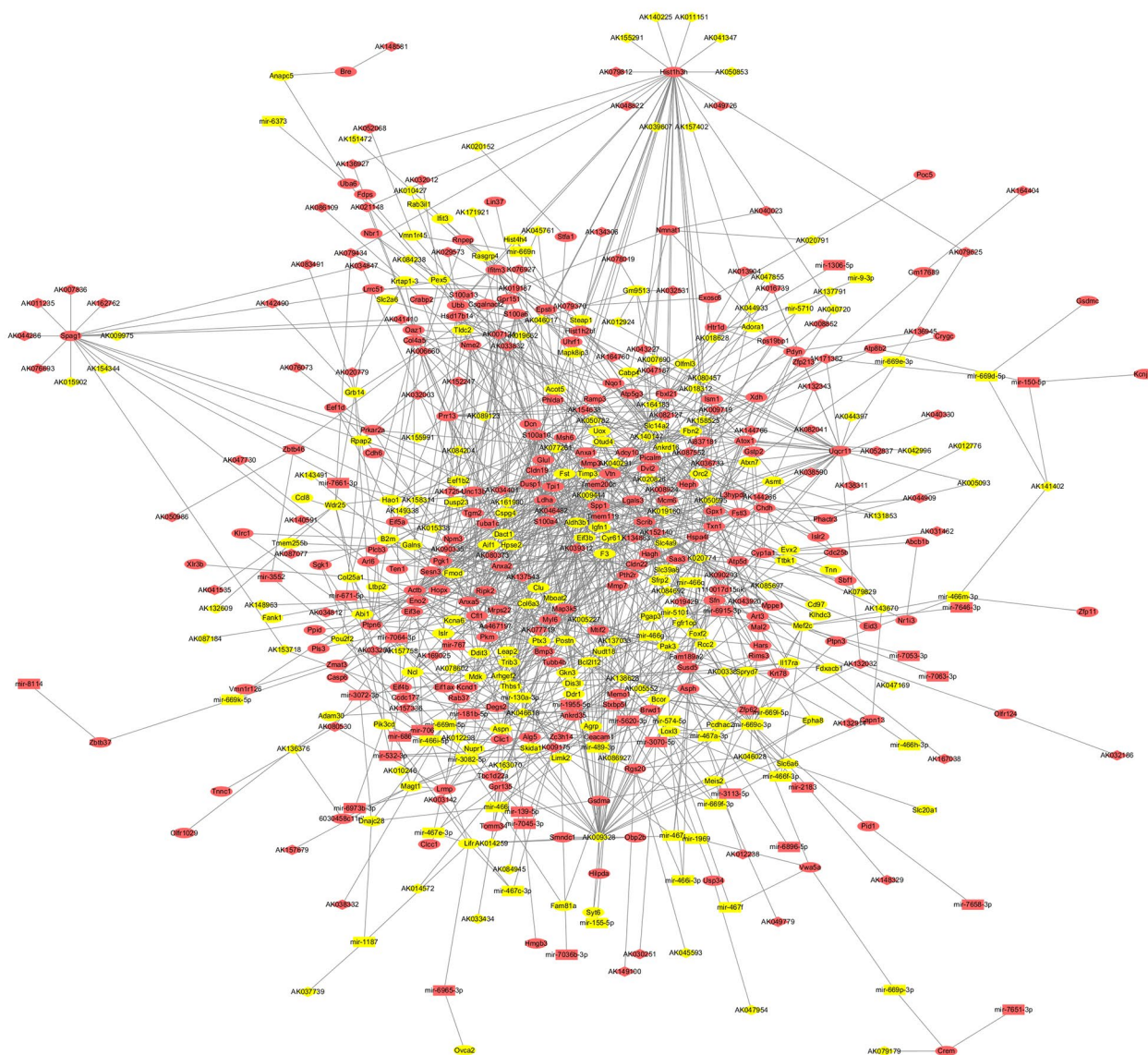


**Fig. 3** The connected interaction network of differently expressed ceRNA. The ellipse nodes represent miRNAs, the rectangle nodes represents mRNAs, and the diamond nodes represents lncRNAs. Red color indicated genes were up regulated and yellow indicated genes were down regulated

targets. Pathway analysis indicated no significant pathway was enriched in the miRNA-regulated genes.

We identified four candidate pathways related to osteoblast proliferation, i.e., fluid shear stress and atherosclerosis, p53 signaling, focal adhesion and PI3k-Akt pathways. A total of 22 miRNAs were involved in these pathways through regulating target genes. For example, six miRNAs (mir-7646-3p, mir-7063-3p, mir-669c-3p, mir-5101, mir-466 m-3p, and mir-466f-3p) were predicted to target *Mef2c* in the PI3K-Akt signaling pathway.

Only four biological processes were significantly enriched in the lncRNA-regulated mRNAs. Among those processes, extracellular matrix organization and extracellular structure organization are involved in the

accumulation of cytoskeletal components [32]. Regarding enriched pathways in the lncRNAs, MAPK signaling and fluid shear stress were identified as two candidate pathways involved in the regulation of osteoblast proliferation.

Of the 1030 dysregulated ceRNAs, 538 interacted with each other (Fig. 3). In addition, some isolated sub-networks only included two components. The core network consisted of 530 nodes and 1 196 connections among ceRNAs, including 181 lncRNAs, 63 miRNAs, and 286 mRNAs. Within this core network, 593 pairs showed positive regulatory associations and 603 pairs showed negative regulatory associations.

**Table 2** The top 10 hub genes with a high degree of connectivity

mRNA	degree	miRNA	degree	lncRNA	degree
Actb	23	mir-669c-3p	13	AK009328	40
Hist1h3h	20	mir-3082-5p	7	AK138628	27
Dcn	17	mir-181b-5p	5	AK020774	26
Lgals3	17	mir-466i-5p	5	AK050595	23
Anxa5	16	mir-467a-3p	5	AK090335	21
Hist1h3h	16	mir-532-3p	5	AK152140	19
Spp1	16	mir-669f-3p	5	AK007124	16
Tpi1	16	mir-130a-3p	4	AK046618	16
Thbs1	15	mir-466f-3p	4	AK087552	16
Tmem200c	14	mir-466j	4	AK019187	15

Degree is the measure of the total number of edges connected to a particular node

Results showed that the *Actb* coding gene had the highest degree among all mRNAs, while AK009328 had the highest degree among all dysregulated RNAs (Table 2). *Actb* also showed the highest closeness centrality and second highest betweenness centrality, indicating a core position in network topology. *Actb* is known to interact with certain genes related to cell proliferation, such as *Txn1*, *Casp6*, and *Arhgef2* [33–35]. Most miRNAs interacted with only 1–2 genes. Mir-669c-3p targeted 13 genes including *Mef2c*. AK009328 had 40 targets that are all coding genes.

### Primary co-regulated pathway in ceRNA network

After functional analysis, the fluid shear stress and atherosclerosis pathway was the most significantly enriched in the entire ceRNA network. Further expression analysis of this pathway was carried out, which identified six up-regulated genes and four down-regulated genes (Fig. 4). Notably, this pathway shares many processes with the focal adhesion, cell apoptosis, PI3k-Akt, MAPK, and NF- $\kappa$ B signaling pathways, which are all related to cell growth [36, 37]. For example, FAK, a key gene in the focal adhesion pathway, is a promoter of osteoblast proliferation [28, 29]. Our results also showed that *Mef2* and *PI3K* in the PI3k-Akt pathway were down-regulated, which may reduce cell proliferation [30]. The MAPK signaling pathway is activated in osteoblasts under fluoride exposure and can stimulate growth [31–33]. No dysregulated genes in the NF- $\kappa$ B signaling and apoptosis pathways were enriched.

### Co-modules of ceRNA related to the fluid shear stress and atherosclerosis pathway

After network-regularized sparse orthogonal-regularized joint non-negative matrix factorization (NSOJNMF), we obtained 200 ceRNA modules, each containing an average of 6.8 mRNAs, 1.7 miRNAs, and 7.9 lncRNAs. If more than one gene in a module participated in the fluid shear stress and atherosclerosis pathway, the module

was considered to be associated with that pathway. For example, genes in co-module 15 involved in the fluid shear stress and atherosclerosis pathway included *Actb* and *Txn1*. Genes, lncRNAs, and miRNAs in the module were highly correlated (Fig. 4). Although other genes in the module are not involved in the fluid shear stress and atherosclerosis pathway, *S100a6* and *Ifitm3* are known to regulate PI3K signaling [38, 39], a sub-pathway of the fluid shear stress and atherosclerosis pathway. In addition, mir-466 h is implicated in apoptosis regulation [40].

### Predicted MACF1 regulation network for MC3T3-E1 osteoblast proliferation

After analysis, we reconstructed the ceRNA network with genes and their interaction ncRNA pairs in the fluid shear stress and atherosclerosis pathway (Fig. 5). We found that MACF1 regulated miRNAs and proliferation-related genes via its targeted genes directly and indirectly. For example, knockdown of MACF1 attenuated the phosphorylation of GSK3 $\beta$ , which regulated transcription factors targeting miRNAs and, in turn, dysregulated the expression of core genes.

Our results also indicated that *Mef2c* plays an important role in the MACF1 regulation network. Firstly, mir-466 m-3p, mir-466f-3p, and mir-5101, which are predicted to inhibit *Mef2c*, were all down-regulated, as was AK141402, which can sponge mir-466 m-3p. In addition, mir-7646-3p and mir-7063-3p were up-regulated, consistent with the down-regulation of *Mef2c*. In mammalian cells, p38 can be regulated by dysregulated MAP3Ks and DUSP1 [41, 42], and p38-catalyzed phosphorylation can increase the transactivation of MEF2C [43, 44].

### Discussion

MACF1 plays an important role in regulating osteoblast proliferation and differentiation in bone-forming osteoblasts [4, 5, 45]. However, no integrated network has been reported regarding its underlying regulatory mechanism.

In recent years, ncRNAs, such as lncRNAs and miRNAs, have emerged as previously underappreciated classes of gene expression modulators that regulate various cellular processes [9–11, 46]. In the current study, we illustrated a comprehensive ceRNA network for MACF1 deletion to regulate osteoblast proliferation through bioinformatics analysis of gene chip data.

In the current study, MACF1 deletion resulted in a large number of differentially expressed RNAs. The most enriched GO terms in the mRNAs and lncRNAs were related to positive regulation of cell death and extracellular matrix organization, which may be related to MACF1 deletion as it binds with F-actin and microtubules [7]. Based on mRNA analysis, the fluid shear stress and atherosclerosis, p53 signaling, and focal adhesion pathways

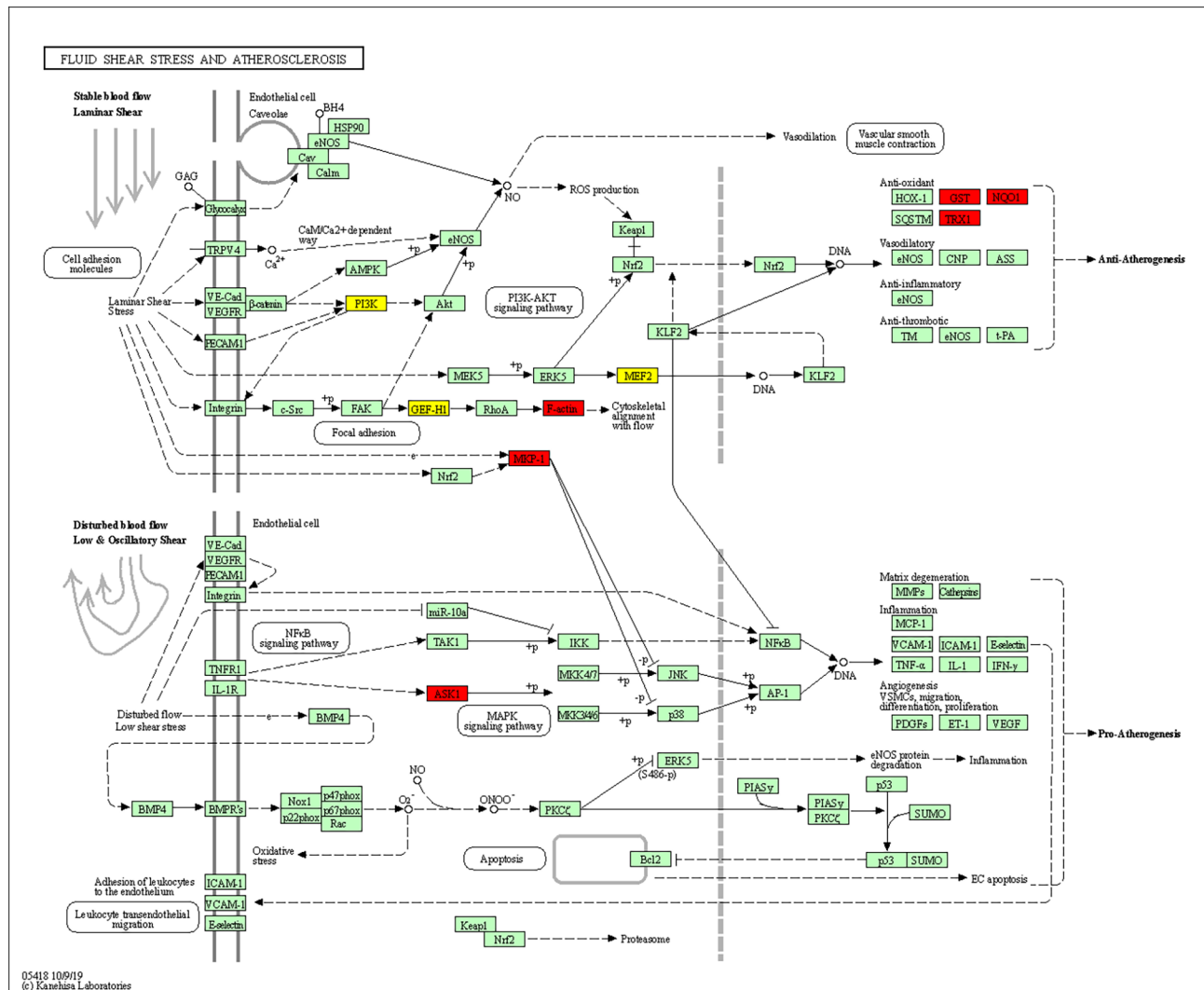


**Fig. 4** Fluid shear stress and atherosclerosis pathway. Red nodes indicated mRNA were up regulated and yellow nodes indicated mRNA were down regulated

promoted osteoblastogenesis. Fluid shear stress plays a critical role in promoting osteoblast proliferation and differentiation [47, 48]. It can promote cytoskeletal reorganization to activate the ERK5 pathway [25, 26, 47]. MACF1 deletion may result in similar cytoskeletal reorganization to regulate osteoblast proliferation. Among the 19 genes mapped to the three pathways in the current work, *Map3k* and *Mef2* are well-studied in osteoblast proliferation [49–52]. *Map3k* participates in MEK1 and MEK2 activation [53]. In turn, MEK1/2 activate ERKs to phosphorylate RUNX2, thereby enhancing the proliferation of osteoblast progenitors. *Mef2* is a component of the enhanceosome that regulates the enhancer of *Runx2* [54]. In addition, the *Txn1*, *Dusp1*, *Nqo1*, *Arhgef2*, *Pik3cd*, *Sfn*, and *Sesn3* genes can regulate cell proliferation too. Five pathways promoting osteoblastogenesis were found to be regulated by miRNAs. In addition to the fluid

shear stress and atherosclerosis pathway, the p53 signaling and focal adhesion pathways were also enriched in differentially expressed mRNAs. Furthermore, the apoptosis and PI3K-Akt signaling pathways were also enriched in the miRNA target genes. Several miRNAs targeting these pathways are reported to influence cell proliferation. For example, although Mir-532-3p inhibits osteogenic differentiation in MC3T3-E1 cells [55], it also inhibits proliferation by regulating  $\beta$ -catenin expression and targeting the phosphatase and tensin homolog (PTEN) gene in the PI3K/AKT signaling pathway [56]. Thus, Mir-532-3p may be a potential regulating factor of osteoblast proliferation following MACF1 deletion. In addition, Mir-466f-3p is down-regulated during osteoblast differentiation and bone regeneration [57] and Mir-139-5p can inhibit mesenchymal stem cell (MSC) osteogenesis through the Wnt/ $\beta$ -catenin pathway by directly targeting CTNNB1

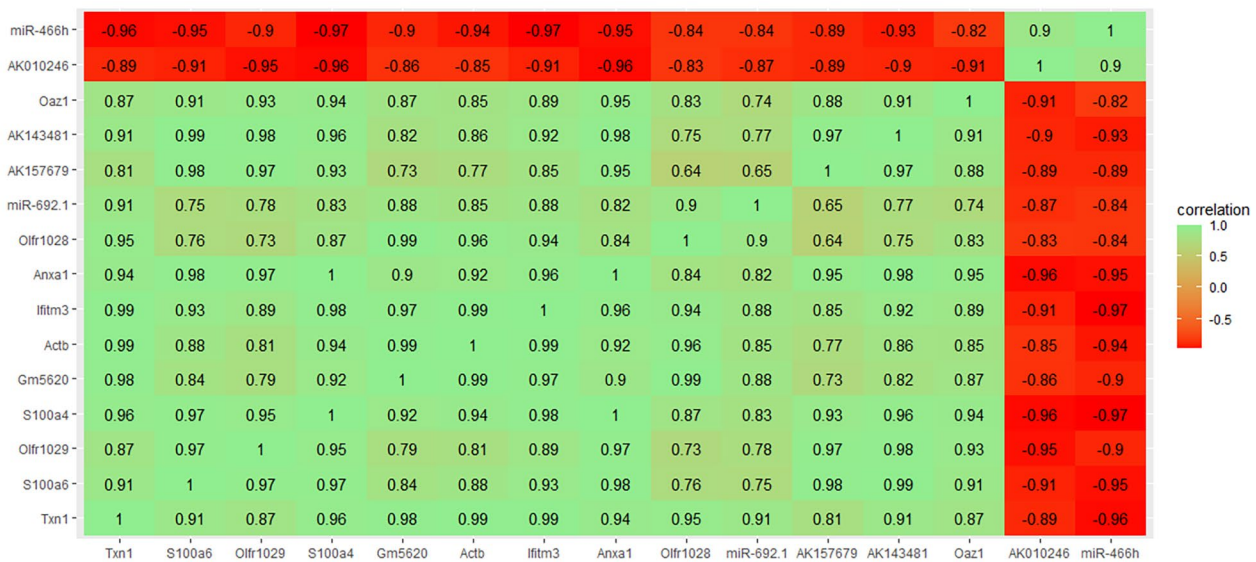


**Fig. 5** Spearman correlation of lncRNAs and mRNAs in ceRNA network. Green (red) indicates positive (negative) correlation

and frizzled 4 (FZD4) [58]. Thus, these miRNAs may also participate in cell proliferation induced by MACF1. We also identified several dysregulated miRNAs that are involved in cell proliferation, although they have not been reported in osteogenesis. For example, Mir-466q modulates the p38 MAPK signaling pathway by inhibiting the expression of its target gene *Map3k* [59]. Mir-574-5p targets *Bcl11a* and *Sox2* to attenuate proliferation in triple-negative breast cancer cells and governs cell proliferation through the Wnt/ $\beta$ -catenin pathway in PTC-1 cells [60]. Mir-489-3p can also inhibit cell proliferation by targeting the brain-derived neurotrophic factor-mediated PI3K/AKT pathway in glioblastoma cells and suppress proliferation by targeting JAG1 in bladder cancer cells [61]. For some miRNAs, such as mir-7646-3p, mir-7045-3p, and mir-6973b-3p, although they have not been implicated in regulating proliferation, our results indicate that they have the potential to influence osteogenesis through their target genes.

The fluid shear stress and atherosclerosis, MAPK signaling, and apoptosis pathways can influence proliferation via lncRNA regulation [26, 47, 48, 53, 62]. Here, four lncRNAs (AK079829, AK079370, AK154638, and AK161980) were predicted to regulate these pathways. Previous research has shown that AK079370 can inhibit bone formation by suppressing the Wnt/ $\beta$ -catenin pathway [63]. Our results also indicated that AK079370 may interact with *Dusp1*, which can inhibit cell proliferation via the ERK signaling pathway [64]. Two cell proliferation genes, *Txn1* and *Map3k5*, were also regulated by AK079829 and AK161980 and by AK154638, respectively. However, their functional mechanisms related to osteoblasts require further experimental validation.

We also identified three interaction pairs (Mir-3082-5p and AK003142, mir-466 m-3p and AK141402, and mir-532-3p and AK009175) that may regulate osteoblastogenesis-related genes. As mentioned above, mir-532-3p has the capacity to inhibit proliferation by regulating  $\beta$ -catenin expression, while mir-466 m-3p is predicted to target *Mef2c* in the PI3K-Akt signaling pathway [56]. In our study, Mir-3082-5p was predicted to target *Pik3* to participate in osteogenesis. However, although several lncRNA-mRNA pairs were identified, none directly participated in proliferation. Thus, lncRNAs appear to regulate osteoblastogenesis by sponging miRNAs rather than by directly regulating mRNAs.

Co-module analysis also revealed that ceRNA network contributed to the cell proliferation. A total of 106 co-modules were found related to fluid shear stress and atherosclerosis pathway. This may be caused by the high degree of connectivity of *Actb*, which is involved in the co-modules and the fluid shear stress and atherosclerosis pathway simultaneously. *Actb* also participates in focal adhesion and adherent junction pathways, two key regulation pathways in osteoblast proliferation. Besides, *Txn1* is involved in co-modules 15,100 and 187. *Txn1* may play an important role in regulating cell proliferation [65]. More importantly, the analysis of co-modules is convenient to find RNAs that could complement the ceRNA regulation network. For example, miR-466 in co-module 187 could significantly inhibit cell proliferation while miR-671-5p in co-module 100 could foster the proliferation [66–68]. The results indicate that ceRNA network plays an important role in the regulation of cell proliferation.

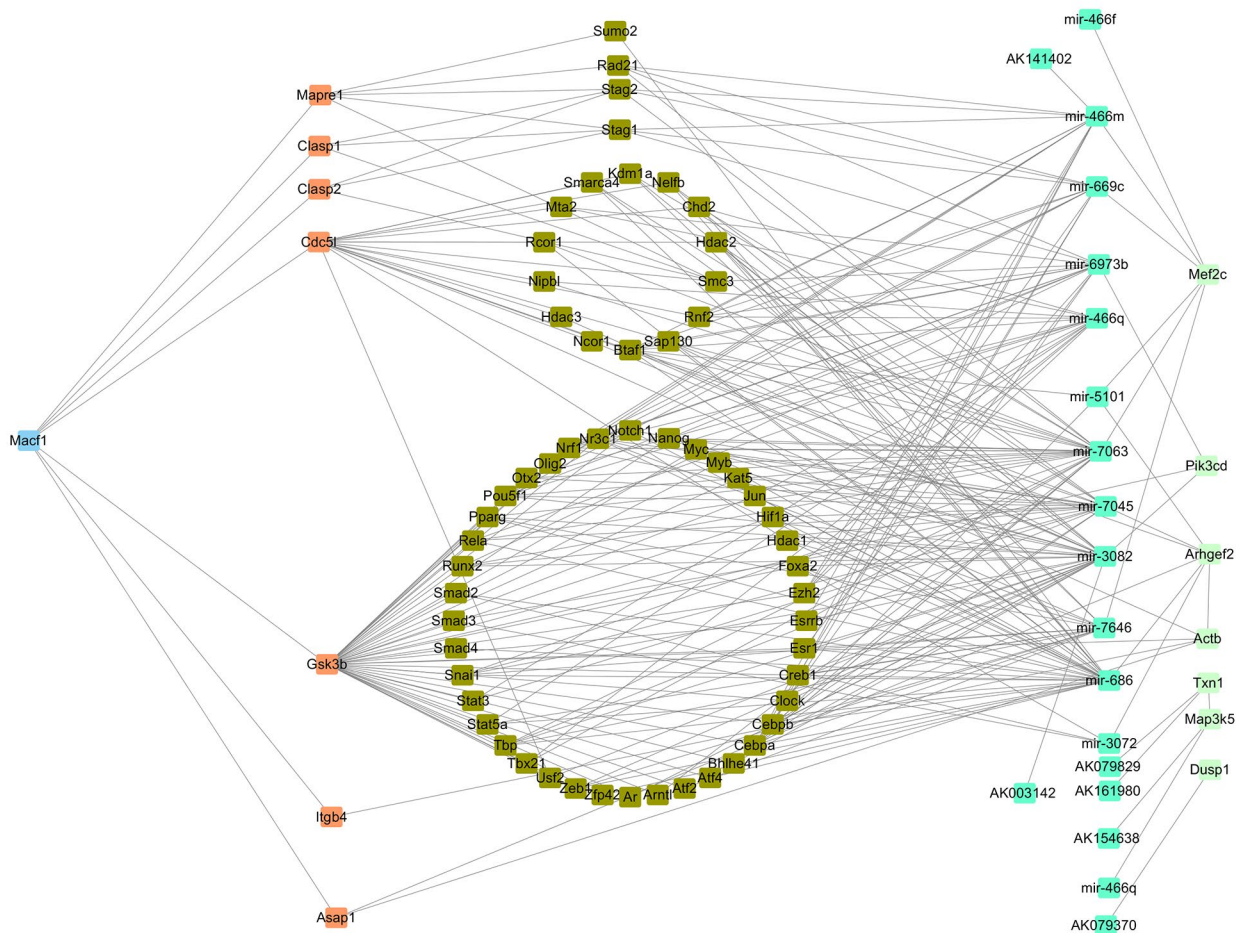


**Fig. 6** Predicted MACF1 regulation network of ceRNA in MC3T3-E1 cells. Orange nodes indicate genes interact with MACF1 directly; olive nodes indicate transcription factors that regulated related miRNAs; aquamarine nodes indicate ncRNA and lightgreen nodes indicate genes enriched in fluid shear stress and atherosclerosis pathway

We found that the fluid shear stress and atherosclerosis pathway was enriched in mRNAs, lncRNAs, and miRNAs simultaneously. Fluid shear stress is thought to mediate bone cell proliferation by producing cellular chemical signals [47]. The extracellular signal-regulated kinase 5 (ERK5) pathway is well-studied in regard to the promotion effects of fluid shear stress on osteoblast proliferation [25, 26, 69]. The fluid shear stress and atherosclerosis pathway shares various processes with the PI3k-AKT signaling, focal adhesion, NF-κB signaling, MAPK signaling pathways, which are key regulation pathways in osteoblast proliferation [27, 28, 49, 50, 52, 53, 70–72]. After we reconstructed the lncRNA and miRNA-regulated pathway for DEGs, all related lncRNAs increased. Core genes in this interaction network included *Pik3ca*, *Mef2a*, *Map3k5*, and *Dusp1*, which are related to cell proliferation [64, 73, 74]. The DEGs revealed that the network contributed to osteoblast proliferation via multiple approaches. For example, AK154638 and AK079370

were predicted to act as antisense lncRNAs for *Map3k5* and *Dusp1*, respectively, to inhibit osteoblast proliferation. Mir-466f-3p, mir-510, mir-466 m-3p, mir-669c, mir-7063, and mir-7646 negatively regulated osteogenesis by binding to *Mef2c*, while AK141402 sponged mir-466 m-3p to resist this inhibition. In previous research, we found that proliferation and differentiation are inhibited in MACF1-knockdown MC3T3-E1 cells [4, 30]. This is consistent with the function of *Mef2c* in cell proliferation and differentiation, which regulates a novel *Runx2* enhancer for osteoblast-specific expression [54]. In our regulation network, only mir-7063 and mir-7646 targeting *mef2c* were increased. Thus, it is possible that MACF1 influences *Mef2c* expression via GSK3β and cell division cycle 5 like (CDC5L), which may target miRNA transcription factors.

Overall, our analysis revealed a comprehensive ceRNA network of MACF1 for the regulation of osteoblast proliferation. Using bioinformatics analysis, a considerable



number of functional ncRNAs were predicted to be involved in the regulation of osteoblast proliferation. The fluid shear stress and atherosclerosis pathway was presumed as the most important pathway for MACF1 to regulate osteogenesis. Although further *in vivo* and *in vitro* experiments are required to test this hypothesis, the present study provides novel insight into the molecular mechanism underlying osteoblast proliferation.

## Materials and methods

### Cell culture and construction of MACF1-knockdown cell line

Murine preosteoblast MC3T3-E1 cell line was generously provided by Dr. Hong Zhou (University of Sydney, Sydney, NSW, Australia). The MC3T3-E1 cells were cultured in  $\alpha$ -modified Eagle's medium ( $\alpha$ -MEM) (Gibco, Carlsbad, CA, USA) supplemented with 10% fetal bovine serum (FBS) (Life Technologies, USA) and 1% penicillin/streptomycin. Cells were incubated for 15 days at 37 °C with 5% CO<sub>2</sub> in a humidified chamber. The MACF1-knockdown cell line was constructed as described in our previous report [4]. In brief, the MC3T3-E1 cells were transfected with short hairpin RNA (shRNA) specifically targeting the murine MACF1 lentivirus vector or with scrambled shRNA, and the stably transfected cell lines were selected using puromycin. After 15 days of selection, all cells were collected for further study.

### LncRNA, miRNA, and mRNA microarray analyses

The collected MC3T3-E1 cells were subjected to sequencing by RiboBio Co., Ltd. (Guangzhou, China) for lncRNA, miRNA, and mRNA microarray analyses. Total RNA was harvested and quantified, and its quantity and purity were assessed using a K5500 Micro-Spectrophotometer (Beijing Kaiuo Technology Development Co., Ltd., Beijing, China). Here, A260/A280  $\geq$  1.5 and A260/A230  $\geq$  1 indicated acceptable RNA purity and RNA integrity number (RIN)  $\geq$  7 (based on an Agilent 2200 RNA assay, Agilent Technologies, USA) indicated acceptable RNA integrity. Genomic DNA contamination was evaluated by gel electrophoresis.

### Differentially expressed mRNAs, miRNAs, and lncRNAs

The fold-change of each differentially expressed mRNA and lncRNA was obtained by log<sub>2</sub> fold-change (normalized spot intensities were transformed to gene expression log<sub>2</sub> ratios between test and control samples). The *P*-values were calculated using analysis of variance (ANOVA). Differentially expressed genes (DEGs) were determined based on fold-change  $>$  2 and adjusted *P*  $<$  0.05.

For lncRNA identification, the transcripts mapped to known genes were eliminated. The Coding Potential Calculator (CPC) and Coding Non-Coding Index (CNCI)

were then used to predict the coding potential of the sequences, requiring CPC and CNCI scores  $<$  0 as indicators for potential lncRNAs.

Finally, differentially expressed mRNAs were selected for cluster analysis performed using the R language package ggplots (v3.3.2) according to Fragments Per Kilobase of exon model per Million mapped fragments (RPKM) values.

### Prediction of target genes of differentially expressed ncRNAs

Based on the co-expression of lncRNAs and mRNAs (correlation 0.99 or  $-0.99$  and *P*  $<$  0.05), the functions of the lncRNAs were executed on coding genes via cis- or trans-regulation. The lncRNAs and target coding genes were considered lncRNA-mRNA pairs. BEDTools (v2.29.1) was used for positional relationship analysis. If the lncRNA gene was within 100 kb upstream or downstream of the coding gene, it was determined to be cis-regulatory, while trans-prediction was based on the binding energy of the lncRNA and coding genes according to sequence complementarity. Pairs of lncRNA and mRNA with a binding  $\Delta G < -0.1$  based on LncTar analysis were deemed interactive.

Target gene prediction for miRNAs was performed using the Encyclopedia of RNA Interactomes (ENCORI) database [75], which provides seven miRNA target gene prediction programs, i.e., PITA, RNA22, miRmap, DIANA-microT, miRanda, PicTar, and TargetScan. The prediction results were screened using at least three program predictions.

To identify the miRNAs that can target lncRNAs, the binding of lncRNAs to miRNAs was predicted using the bioinformatics tool starBase with ENCORI APIs [75].

### Construction and analysis of lncRNA, miRNA, and mRNA interaction network

lncRNAs can target mRNAs through cis or trans activity. Coupled with the targeted relationship between miRNAs and mRNAs and possible targeted relationship between miRNAs and lncRNAs, lncRNA-miRNA-mRNA network interactions were identified using STRING (v11). Results were visualized using Cytoscape (v3.6.0) [76]. In the network diagram, connections indicate possible regulatory relationships. Core genes were detected using NetworkAnalyzer (v2.8) by calculating network topology parameters.

### Functional enrichment analysis

To determine the functional modules, we focused on the DEGs and ncRNAs and conducted functional enrichment analysis with clusterProfiler [77]. For ncRNAs, target genes were used for analysis. Gene Ontology (GO) and Kyoto Encyclopedia of Genes and Genomes (KEGG)

pathway enrichment analyses were screened at  $P < 0.05$  and  $q$ -value  $< 0.05$ .

### Recognition of ceRNA co-modules

After identifying functional modules, to further discover their potential biological associations, we applied network-regularized sparse orthogonal-regularized joint non-negative matrix factorization (NSOJNMF) to identify correlative modules using multi-dimensional genomics data [78–80]. The code is public available at <https://github.com/JN-WYJ/NSOJNMF>. Briefly, the three microarray data X1, X2 and X3 were decomposed into a common basis matrix  $W \in \mathbb{R}^{m \times K}$ , and different coefficient matrices  $H_i \in \mathbb{R}^{K \times n_i}$  ( $i=1,2,3$ ) using the JNMF framework. The prior knowledge of the algorithm combination includes the known or predicted interactions of the three RNAs as described in the previous section. Z-score of each column was used in the coefficient matrix to select the members. Eventually,  $k$  ceRNA co-modules can be identified.  $K$  was assigned to 200 according to the number of the mRNA enrichment pathways in this study. The constraint parameters were  $\lambda_1 = \lambda_2 = 0.001$ . The sparse parameter  $\gamma = 10$  and maximum number of iterations to run is 500. Matlab (R2021a) was used to calculate the co-modules, with the selection of co-module number set to 200. The constraint parameters were  $\lambda = 0.001$  and  $\gamma = 10$ .

### Re-construction of ceRNA regulation pathway for proliferation in MACF1 deletion cells

To build a MACF1-regulated ceRNA network, STRING and TransmiR (v2.0) were used to predict the relationship between the core ceRNAs and MACF1. Firstly, direct target genes of MACF1 were extended by STRING and transcription factors of miRNA were predicted by TransmiR, respectively. The MACF1-target network and TF-miRNA network were then integrated into a sub-network of a previously built ceRNA network of core genes. Thus, a MACF1-TF-miRNA-mRNA network was constructed.

### Supplementary information

The online version contains supplementary material available at <https://doi.org/10.1186/s12864-022-08910-0>.

Supplementary Material 1

### Acknowledgements

The authors thank all the participants and instructors who participated in the study.

### Authors' information

<sup>1</sup>Lab for Bone Metabolism, Key Lab for Space Biosciences and Biotechnology, Xi'an Key Laboratory of Special Medicine and Health Engineering, Research Center for Special Medicine and Health Systems Engineering, NPU-UAB Joint Laboratory for Bone Metabolism, School of Life Sciences, Northwestern Polytechnical University, Xi'an, Shaanxi, 710072, China.

<sup>2</sup>Department of Clinical Laboratory, Academician (expert) workstation, Lab of epigenetics and RNA therapy, Affiliated Hospital of North Sichuan Medical College, Nanchong 637000, P.R.China.

### Authors' contributions

Shanfeng Jiang and Airong Qian designed the study. Chong Yin and Kai Dang performed the biological experiments. Shanfeng Jiang, Ying Huai and Wenjuan Zhang performed bioinformatics analysis. Shanfeng Jiang prepared the draft of the manuscript. All authors read and approved the final manuscript.

### Funding

This study was supported by the National Natural Science Foundation of China (31570940) and the Fundamental Research Funds for the Central Universities No. D5000210746.

### Data availability

mRNA and lncRNA arrays data have been deposited in the ArrayExpress database at EMBL-EBI ([www.ebi.ac.uk/arrayexpress](http://www.ebi.ac.uk/arrayexpress)) under accession number E-MTAB-11,425 and E-MTAB-11,426, respectively. miRNA data is available at: <https://www.ncbi.nlm.nih.gov/geo/query/acc.cgi?acc=GSE202962> (reviewer token: cvalwmqkbhsdbqp). The datasets used and/or analyzed during the current study are available from the corresponding author on reasonable request.

### Declarations

#### Ethics approval and consent to participate

Not applicable.

#### Consent for publication

Not applicable.

#### Competing interests

The authors declare they have no competing interests.

Received: 20 April 2022 / Accepted: 26 September 2022

Published online: 07 October 2022

### References

- Saad FA. Novel insights into the complex architecture of osteoporosis molecular genetics. *Ann N Y Acad Sci.* 2020;1462(1):37–52.
- An J, Yang H, Zhang Q, Liu C, Zhao J, Zhang L, Chen B. Natural products for treatment of osteoporosis: The effects and mechanisms on promoting osteoblast-mediated bone formation. *Life Sci.* 2016;147:46–58.
- Marie PJ. Targeting integrins to promote bone formation and repair. *Nat Rev Endocrinol.* 2013;9(5):288–95.
- Hu L, Su P, Li R, Yan K, Chen Z, Shang P, Qian A. Knockdown of microtubule actin crosslinking factor 1 inhibits cell proliferation in MC3T3-E1 osteoblastic cells. *BMB Rep.* 2015;48(10):583–8.
- Yin C, Zhang Y, Hu L, Tian Y, Chen Z, Li D, Zhao F, Su P, Ma X, Zhang G, et al: Mechanical unloading reduces microtubule actin crosslinking factor 1 expression to inhibit  $\beta$ -catenin signaling and osteoblast proliferation. 2018, 233(7):5405–5419.
- Leung CL, Sun D, Zheng M, Knowles DR, Liem RK. Microtubule actin cross-linking factor (MACF): a hybrid of dystonin and dystrophin that can interact with the actin and microtubule cytoskeletons. *J Cell Biol.* 1999;147(6):1275–86.
- Karakesisoglou I, Yang Y, Fuchs E. An epidermal plakin that integrates actin and microtubule networks at cellular junctions. *J Cell Biol.* 2000;149(1):195–208.
- Karner CM, Long F. Wnt signaling and cellular metabolism in osteoblasts. 2017, 74(9):1649–1657.
- Chen Y, Lin Y, Bai Y, Cheng D, Bi Z. A Long Noncoding RNA (lncRNA)-Associated Competing Endogenous RNA (ceRNA) Network Identifies Eight lncRNA Biomarkers in Patients with Osteoarthritis of the Knee. *Med Sci Monit.* 2019;25:2058–65.
- Slack FJ, Chinnaiyan AM. The Role of Non-coding RNAs in Oncology. *Cell.* 2019;179(5):1033–55.
- Esteller M. Non-coding RNAs in human disease. *Nat Rev Genet.* 2011;12(12):861–74.
- Bushati N, Cohen SM. microRNA functions. *Annu Rev Cell Dev Biol.* 2007;23:175–205.

13. Mohr AM, Mott JL. Overview of microRNA biology. *Semin Liver Dis.* 2015;35(1):3–11.
14. Saliminejad K, Khorram Khorshid HR, Soleymani Fard S, Ghaffari SH: An overview of microRNAs: Biology, functions, therapeutics, and analysis methods. 2019, 234(5):5451–5465.
15. Zhu S, Yao F, Qiu H, Zhang G, Xu H, Xu J. Coupling factors and exosomal packaging microRNAs involved in the regulation of bone remodelling. *Biol Rev Camb Philos Soc.* 2018;93(1):469–80.
16. Chang M, Lin H, Fu H, Wang B, Han G, Fan M. MicroRNA-195-5p Regulates Osteogenic Differentiation of Periodontal Ligament Cells Under Mechanical Loading. *J Cell Physiol.* 2017;232(12):3762–74.
17. Kuang W, Zheng L, Xu X, Lin Y, Lin J, Wu J, Tan J. Dysregulation of the miR-146a-Smad4 axis impairs osteogenesis of bone mesenchymal stem cells under inflammation. *Bone Res.* 2017;5:17037.
18. Liao L, Yang X, Su X, Hu C, Zhu X, Yang N, Chen X, Shi S, Shi S, Jin Y. Redundant miR-3077-5p and miR-705 mediate the shift of mesenchymal stem cell lineage commitment to adipocyte in osteoporosis bone marrow. *Cell Death Dis.* 2013;4(4):e600.
19. Ren LR, Yao RB, Wang SY, Gong XD, Xu JT, Yang KS. MiR-27a-3p promotes the osteogenic differentiation by activating CRY2/ERK1/2 axis. 2021, 27(1):43.
20. Xu D, Gao Y, Hu N, Wu L, Chen Q. miR-365 Ameliorates Dexamethasone-Induced Suppression of Osteogenesis in MC3T3-E1 Cells by Targeting HDAC4. *Int J Mol Sci* 2017, 18(5).
21. Kopp F, Mendell JT. Functional Classification and Experimental Dissection of Long Noncoding RNAs. *Cell.* 2018;172(3):393–407.
22. Sun Y, Cai M, Zhong J, Yang L, Xiao J, Jin F, Xue H, Liu X, Liu H, Zhang Y, et al: The long noncoding RNA Inc-ob1 facilitates bone formation by upregulating Osterix in osteoblasts. 2019, 1(4):485–496.
23. Gong YY, Peng MY, Yin DQ, Yang YF. Long non-coding RNA H19 promotes the osteogenic differentiation of rat ectomesenchymal stem cells via Wnt/ $\beta$ -catenin signaling pathway. *Eur Rev Med Pharmacol Sci.* 2018;22(24):8805–13.
24. Zhou P, Li Y, Di R, Yang Y, Meng S, Song F, Ma L. H19 and Foxc2 synergistically promotes osteogenic differentiation of BMSCs via Wnt- $\beta$ -catenin pathway. 2019, 234(8):13799–13806.
25. Bo Z, Bin G, Jing W, Cui Fang W, Liping A, Jinglin M, Jin J, Xiaoyi T, Cong C, Ning D, et al. Fluid shear stress promotes osteoblast proliferation via the Gq-ERK5 signaling pathway. *Connect Tissue Res.* 2016;57(4):299–306.
26. Ding N, Geng B, Li Z, Yang Q, Yan L, Wan L, Zhang B, Wang C, Xia Y. Fluid shear stress promotes osteoblast proliferation through the NFATc1-ERK5 pathway. *Connect Tissue Res.* 2019;60(2):107–16.
27. Horikiri Y, Shimo T, Kurio N, Okui T, Matsumoto K, Iwamoto M, Sasaki A. Sonic hedgehog regulates osteoblast function by focal adhesion kinase signaling in the process of fracture healing. *PLoS ONE.* 2013;8(10):e76785.
28. Lopes HB, Souza ATP. Effect of focal adhesion kinase inhibition on osteoblastic cells grown on titanium with different topographies. 2020, 28:e20190156.
29. Zhang M, Xie Y, Zhou Y, Chen X, Xin Z, An J, Hou J, Chen Z. Exendin-4 enhances proliferation of senescent osteoblasts through activation of the IGF-1/IGF-1R signaling pathway. *Biochem Biophys Res Commun.* 2019;516(1):300–6.
30. Hu L, Yin C, Chen D. MACF1 promotes osteoblast differentiation by sequestering repressors in cytoplasm. 2021, 28(7):2160–2178.
31. Akula S, Brosch IK, Leipzig ND. Fluorinated Methacrylamide Chitosan Hydrogels Enhance Cellular Wound Healing Processes. 2017, 45(11):2693–2702.
32. Zamir E, Geiger B. Molecular complexity and dynamics of cell-matrix adhesions. *J Cell Sci.* 2001;114(Pt 20):3583–90.
33. Sofi MH, Wu Y, Schutt SD, Dai M, Daenthansanmak A, Heinrichs Voss J, Nguyen H, Bastian D, Iamsawat S, Selvam SP, et al. Thioredoxin-1 confines T cell alloresponse and pathogenicity in graft-versus-host disease. *J Clin Invest.* 2019;129(7):2760–74.
34. Gauthier-Fisher A, Lin DC, Greeve M, Kaplan DR, Rottapel R, Miller FD. Lfc and Tctex-1 regulate the genesis of neurons from cortical precursor cells. *Nat Neurosci.* 2009;12(6):735–44.
35. Kratochvílová A, Veselá B, Ledvína V, Švandová E, Klepárník K, Dadáková K, Beneš P, Matalová E. Osteogenic impact of pro-apoptotic caspase inhibitors in MC3T3-E1 cells. *Sci Rep.* 2020;10(1):7489.
36. Kanehisa M, Goto S. KEGG: kyoto encyclopedia of genes and genomes. *Nucleic Acids Res.* 2000;28(1):27–30.
37. Kanehisa M, Furumichi M, Sato Y, Ishiguro-Watanabe M, Tanabe M. KEGG: integrating viruses and cellular organisms. *Nucleic Acids Res.* 2021;49(D1):D545–d551.
38. Donato R, Sorci G, Giambanco I. S100A6 protein: functional roles. (1420–9071 (Electronic)).
39. Lee J, Robinson MA-O, Ma N, Artadji DA-O, Ahmed MA-O, Xiao G, Sadras T, Deb G, Winchester J, Cosgun KN, et al: IFITM3 functions as a PIP3 scaffold to amplify PI3K signalling in B cells. (1476–4687 (Electronic)).
40. Druz A, Chu C, Fau - Majors B, Majors B, Fau - Sanctuary R, Sanctuary R, Fau - Betenbaugh M, Betenbaugh M, Fau - Shiloach J, Shiloach J. A novel microRNA mmu-miR-466 h affects apoptosis regulation in mammalian cells. (1097 – 0290 (Electronic)).
41. Cronan MR, Nakamura K, Johnson NL, Granger DA, Cuevas BD, Wang JG, Mackman N, Scott JE, Dohman HG, Johnson GL. Defining MAP3 kinases required for MDA-MB-231 cell tumor growth and metastasis. *Oncogene.* 2012;31(34):3889–900.
42. Shen J, Zhang Y, Yu H, Shen B, Liang Y, Jin R, Liu X, Shi L, Cai X. Role of DUSP1/MKP1 in tumorigenesis, tumor progression and therapy. *Cancer Med.* 2016;5(8):2061–8.
43. Han J, Jiang Y, Li Z, Kravchenko VV, Ulevitch RJ. Activation of the transcription factor MEF2C by the MAP kinase p38 in inflammation. *Nature.* 1997;386(6622):296–9.
44. Han J, Molkenkin JD. Regulation of MEF2 by p38 MAPK and its implication in cardiomyocyte biology. *Trends Cardiovasc Med.* 2000;10(1):19–22.
45. Zhang Y, Yin C, Hu L, Chen Z, Zhao F, Li D, Ma J, Ma X, Su P, Qiu W, et al. MACF1 Overexpression by Transfecting the 21 kbp Large Plasmid PEGFP-C1A-ACF7 Promotes Osteoblast Differentiation and Bone Formation. *Hum Gene Ther.* 2018;29(2):259–70.
46. Hou Q, Huang Y, Liu Y, Luo Y, Wang B, Deng R, Zhang S, Liu F, Chen D. Profiling the miRNA-mRNA-lncRNA interaction network in MSC osteoblast differentiation induced by (+)-cholesten-3-one. *BMC Genomics.* 2018;19(1):783.
47. Kapur S, Baylink DJ, Lau KH. Fluid flow shear stress stimulates human osteoblast proliferation and differentiation through multiple interacting and competing signal transduction pathways. *Bone.* 2003;32(3):241–51.
48. Yu W, Qu H, Hu G, Zhang Q, Song K, Guan H, Liu T, Qin J. A microfluidic-based multi-shear device for investigating the effects of low fluid-induced stresses on osteoblasts. *PLoS ONE.* 2014;9(2):e89966.
49. Datta NS, Kolailat R, Fite A, Pettway G, Abou-Samra AB. Distinct roles for mitogen-activated protein kinase phosphatase-1 (MKP-1) and ERK-MAPK in PTH1R signaling during osteoblast proliferation and differentiation. *Cell Signal.* 2010;22(3):457–66.
50. Luo XH, Guo LJ, Yuan LQ, Xie H, Zhou HD, Wu XP, Liao EY. Adiponectin stimulates human osteoblasts proliferation and differentiation via the MAPK signaling pathway. *Int J Mol Sci.* 2005;309(1):99–109.
51. Qiao X, Nie Y, Ma Y, Chen Y, Cheng R, Yin W, Hu Y, Xu W, Xu L. Irisin promotes osteoblast proliferation and differentiation via activating the MAP kinase signaling pathways. *Sci Rep.* 2016;6:18732.
52. Zhu WQ, Yu YJ, Xu LN, Ming PP, Shao SY, Qiu J. Regulation of osteoblast behaviors via cross-talk between Hippo/YAP and MAPK signaling pathway under fluoride exposure. 2019, 97(7):1003–1017.
53. Greenblatt MB, Shim JH, Glimcher LH. Mitogen-activated protein kinase pathways in osteoblasts. *Annu Rev Cell Dev Biol.* 2013;29:63–79.
54. Kawane T, Komori H, Liu W, Moriishi T, Miyazaki T, Mori M, Matsuo Y, Takada Y, Izumi S, Jiang Q, et al. Dlx5 and mef2 regulate a novel runx2 enhancer for osteoblast-specific expression. *J Bone Miner Res.* 2014;29(9):1960–9.
55. Fan Q, Li Y, Sun Q, Jia Y, He C, Sun T. miR-532-3p inhibits osteogenic differentiation in MC3T3-E1 cells by downregulating ETS1. *Biochem Biophys Res Commun.* 2020;525(2):498–504.
56. Liu Y, Li Q, Dai Y, Jiang T, Zhou Y. miR-532-3p Inhibits Proliferation and Promotes Apoptosis of Lymphoma Cells by Targeting  $\beta$ -Catenin. *J Cancer.* 2020;11(16):4762–70.
57. Gong Y, Xu F, Zhang L, Qian Y, Chen J, Huang H, Yu Y. MicroRNA expression signature for Satb2-induced osteogenic differentiation in bone marrow stromal cells. *Mol Cell Biochem.* 2014;387(1–2):227–39.
58. Long H, Sun B, Cheng L, Zhao S, Zhu Y, Zhao R, Zhu J. miR-139-5p Represses BMSC Osteogenesis via Targeting Wnt/ $\beta$ -Catenin Signaling Pathway. *DNA Cell Biol.* 2017;36(8):715–24.
59. Giunti D, Marini C, Parodi B, Usai C, Milanese M, Bonanno G, Kerlero de Rosbo N, Uccelli A. Role of miRNAs shuttled by mesenchymal stem cell-derived small extracellular vesicles in modulating neuroinflammation. *Sci Rep.* 2021;11(1):1740.
60. Wang X, Lu X, Geng Z, Yang G, Shi Y. LncRNA PTCSC3/miR-574-5p Governs Cell Proliferation and Migration of Papillary Thyroid Carcinoma via Wnt/ $\beta$ -Catenin Signaling. *J Cell Biochem.* 2017;118(12):4745–52.
61. Li J, Qu W, Jiang Y, Sun Y, Cheng Y, Zou T, Du S. miR-489 Suppresses Proliferation and Invasion of Human Bladder Cancer Cells. *Oncol Res.* 2016;24(6):391–8.

62. Lv C, Wang L, Zhu X, Lin W, Chen X, Huang Z, Huang L, Yang S. Glucosamine promotes osteoblast proliferation by modulating autophagy via the mammalian target of rapamycin pathway. *Biomed Pharmacother.* 2018;99:271–7.
63. Yin C, Tian Y, Yu Y, Li D, Miao Z, Su P, Zhao Y, Wang X, Pei J, Zhang K, et al. Long noncoding RNA AK039312 and AK079370 inhibits bone formation via miR-199b-5p. *Pharmacol Res.* 2021;163:105230.
64. Yang J, Sun L, Han J, Zheng W, Peng W. DUSP1/MKP-1 regulates proliferation and apoptosis in keratinocytes through the ERK/Elk-1/Egr-1 signaling pathway. *Life Sci.* 2019;223:47–53.
65. Lu T, Zong M, Fan S, Lu Y, Yu S, Fan L. Thioredoxin 1 is associated with the proliferation and apoptosis of rheumatoid arthritis fibroblast-like synoviocytes. *Clin Rheumatol.* 2018;37(1):117–25.
66. Li H, Dong W, Hou J, He D. LINC 01436 is overexpressed in colorectal cancer and promotes cancer cell proliferation by suppressing tumor-suppressive miR-466 maturation. *In Vitro Cell Dev Biol Anim.* 2022;58(2):109–15.
67. Vierthaler M, Sun Q, Wang Y, Steinfass T, Poelchen J, Hielscher T, Novak D, Umansky V, Utikal J, Chen X, et al. ADCK2 Knockdown Affects the Migration of Melanoma Cells via MYL6 miR-671-5p Promotes Cell Proliferation, Invasion, and Migration in Hepatocellular Carcinoma through Targeting ALDH2. *Cancers (Basel).* 2022;14(4):73–82.
68. Xiao Y, Zhang SJ, Yan X, Wu C, Liu QW, Dong HX, Wang LJ, Hu Y. MiR-466 as a poor prognostic predictor suppresses cell proliferation and EMT in breast cancer cells by targeting PSMA7. *Eur Rev Med Pharmacol Sci.* 2021;25(18):5625–35.
69. Yu L, Ma X, Sun J, Tong J, Shi L, Sun L, Zhang J. Fluid shear stress induces osteoblast differentiation and arrests the cell cycle at the G0 phase via the ERK1/2 pathway. *Mol Med Rep.* 2017;16(6):8699–708.
70. Ma H, Ma JX, Xue P, Gao Y, Li YK. Osteoblast proliferation is enhanced upon the insulin receptor substrate 1 overexpression via PI3K signaling leading to down-regulation of NFκB and BAX pathway. *J Mol Med (Berl).* 2015;123(2):126–31.
71. Pan JM, Wu LG, Cai JW, Wu LT, Liang M. Dexamethasone suppresses osteogenesis of osteoblast via the PI3K/Akt signaling pathway in vitro and in vivo. *J Recept Signal Transduct Res.* 2019;39(1):80–6.
72. Sun C, Yuan H, Wang L, Wei X, Williams L, Krebsbach PH, Guan JL, Liu F. FAK Promotes Osteoblast Progenitor Cell Proliferation and Differentiation by Enhancing Wnt Signaling. *J Bone Miner Res.* 2016;31(12):2227–38.
73. Cui H, Han G, Sun B, Fang X, Dai X, Zhou S, Mao H, Wang B. Activating PIK3CA mutation promotes osteogenesis of bone marrow mesenchymal stem cells in macrodactyly. 2020, 11(7):505.
74. Leupin O, Kramer I, Collette NM, Loots GG, Natt F, Kneissel M, Keller H. Control of the SOST bone enhancer by PTH using MEF2 transcription factors. *J Bone Miner Res.* 2007;22(12):1957–67.
75. Li JH, Liu S, Zhou H, Qu LH, Yang JH. starBase v2.0: decoding miRNA-ceRNA, miRNA-ncRNA and protein-RNA interaction networks from large-scale CLIP-Seq data. *Nucleic Acids Res.* 2014;42(Database issue):D92–7.
76. Shannon P, Markiel A, Ozier O, Baliga NS, Wang JT, Ramage D, Amin N, Schwikowski B, Ideker T. Cytoscape: a software environment for integrated models of biomolecular interaction networks. *Genome Res.* 2003;13(11):2498–504.
77. Yu G, Wang LG, Han Y, He QY. clusterProfiler: an R package for comparing biological themes among gene clusters. *Omics.* 2012;16(5):284–7.
78. Zhang S, Liu CC, Li W, Shen H, Laird PW, Zhou XJ. Discovery of multi-dimensional modules by integrative analysis of cancer genomic data. *Nucleic Acids Res.* 2012;40(19):9379–91.
79. Wang Y, Zhou G, Guan T, Wang Y, Xuan C, Ding T, Gao J. A network-based matrix factorization framework for ceRNA co-modules recognition of cancer genomic data. *Brief Bioinform* 2022.
80. Deng J, Kong W, Wang S, Mou X, Zeng W. Prior Knowledge Driven Joint NMF Algorithm for ceRNA Co-Module Identification. *Int J Biol Sci.* 2018;14(13):1822–33.

### Publisher's note

Springer Nature remains neutral with regard to jurisdictional claims in published maps and institutional affiliations.